Eur Biophys J (2001) 30: 17–26
DOI 10.1007/s002490000119

ARTICLE

Yoriko Iwanaga · Dieter Braun · Peter Fromherz

No correlation of focal contacts and close adhesion by comparing GFP-vinculin and fluorescence interference of DiI

Received: 4 April 2000 / Revised version: 29 September 2000 / Accepted: 12 October 2000 / Published online: 2 February 2001

Abstract In regions of focal adhesion, cells adhere to a substrate through the interaction of extracellular matrix proteins and transmembrane integrins which are coupled to the cell skeleton. It is generally assumed that the plasma membrane is brought to close proximity to the substrate there. We used the novel method of fluorescence interference contrast (FLIC) microscopy to measure the distance of the plasma membrane of GD25 fibroblasts on silica coated with fibronectin. We correlated the distance map with the distribution of vinculin tagged with green fluorescent protein. We found that the major part of the membrane was separated by 50 nm from the substrate. With respect to this plateau, we found spots of upward deformation and of close adhesion as well as a general ruffling of the membrane. There was no correlation between the areas of close adhesion and the distribution of vinculin. We conclude that focal adhesion does not imply a close attachment of membrane and substrate.

Key words Cell adhesion · Focal contact · Fibronectin · Vinculin · Green fluorescent protein

Abbreviations *DiI*: 1,1′-dioctadecyl-3,3,3′,3′-tetramethylindocarbocyanine perchlorate · *ECM*: extracellular matrix · *FLIC*: fluorescence interference contrast · *GFP*: green fluorescent protein · *IRM*: interference reflection microscopy · *RICM*: reflection interference contrast microscopy · *TEM*: transmission electron microscopy · *TIRAF*: total internal reflection aqueous fluorescence · *TIRFM*: total internal reflection fluorescence microscopy

Y. Iwanaga · D. Braun · P. Fromherz (✉)
Department of Membrane and Neurophysics,
Max-Planck-Institute for Biochemistry,
82152 Martinsried/Munich, Germany
E-mail: fromherz@biochem.mpg.de
Tel.: +49-89-85782820
Fax: +49-89-85782822

Introduction

Focal adhesion complexes are specialized areas of the plasma membrane where the attachment of fibroblasts to a solid substrate takes place. In these regions, actin filaments converge via distinct cytoskeletal anchor molecules on clustered integrins, which interact with extracellular matrix proteins. The function of the focal adhesion complex in mediating both cell adhesion and transmembrane signaling has been investigated extensively (Richardson and Steiner 1995; Yamada and Geiger 1997). Recent findings have lead to classification of a new type of cell-matrix adhesion (Zamir et al. 2000). To correlate the biochemical studies with structure, the geometry of cell adhesion has to be known under the unperturbed conditions of cell culture.

It is generally accepted that the distance between the plasma membrane of a cultured cell and a solid substrate is narrowed down to 10–15 nm at a focal contact (Alberts et al. 1989). This concept of close adhesion at focal contacts relies on studies by interference reflection microscopy (IRM) (Curtis 1964; Izzard and Lochner 1976; Gingell and Todd 1979) and transmission electron microscopy (TEM) (Chen and Singer 1982). A correlation of the spots of low reflectance of IRM with focal complexes was demonstrated by immunofluorescence of vinculin (Geiger 1979). Roughness of attached membranes was observed also by total internal reflection fluorescence microscopy (TIRFM) (Lanni et al. 1985; Burmeister et al. 1994). Though IRM, TEM, and TIRFM are able to visualize focal contacts, it is notoriously difficult to evaluate the absolute distance of cell and substrate: 1. The spots of low reflection seen by IRM can be explained by optically dense regions at the cytoplasmic side of a focal contact (Heath and Dunn 1978; Bailey and Gingell 1988). 2. Fixation and embedding in a polymer matrix may give rise to local shrinking artifacts both along and perpendicular to the substrate in electron microscopy. 3. The calibration of TIRFM is affected by stray light and adjustment

problems (Gingell and Heavens 1996; Burmeister et al. 1998).

In the present study we reconsidered the geometry of focal adhesion on fibronectin and laminin. We used two cell lines derived from the mouse embryonic stem cell G201 with well-defined cell-matrix interactions that form classical focal contacts: 1. GD25 cells are deficient in the β_1 integrin subunit (Fässler et al. 1995). Their interaction with fibronectin is mediated by $\alpha_V\beta_3$ integrin. They are unable to adhere to laminin. 2. In GD25-β1A cells the integrin subunit β_1 (splice variant A) is reintroduced by stable transfection (Wennerberg et al. 1996). The interaction with fibronectin is still dominated by $\alpha_V\beta_3$ integrin. Binding to laminin is mediated by $\alpha_6\beta_1$ integrin. When $\alpha_V\beta_3$ is blocked with the peptide GRGDS, fibronectin binds to $\alpha_5\beta_1$ integrin. We visualized the focal complexes in situ without fixation and antibody staining by transfecting GD25 and GD25-β1A cells with vinculin which was tagged at its amino terminal with green fluorescent protein (GFP).

We measured the separation of the plasma membrane and the substrate with the novel method of fluorescence interference contrast (FLIC) microscopy (Lambacher and Fromherz 1996; Braun and Fromherz 1997). In FLIC microscopy, cells are cultured on a silicon chip with defined terraces of silicon dioxide. The plasma membrane is labeled with the fluorescent cyanine dye 1,1′-dioctadecyl-3,3,3′,3′-tetramethylindocarbocyanine-perchlorate (DiI, $DiIC_{18}$). Because silicon is a mirror, the fluorescence intensity of a dye depends on its distance from the surface. This is due to the interference between the incident and reflected illumination and due to the interference between the direct and reflected emission light. With appropriate calibration, the intensity can be used to determine the distance with a precision of 1 nm. FLIC microscopy combines the advantages of TIRFM and IRM: the specific labeling of the membrane and the precision of an interference method. On the other hand, the ill-defined optical properties of the cell – that seriously affect the evaluation of IRM and TIRFM – are irrelevant owing to the dominating effect of the well-defined silicon/silicon dioxide interface. Difficult optical adjustments – that affect multi-angle TIRFM – are not required owing to an internal calibration on a microstructured silicon chip.

Materials and methods

Cells with GFP-vinculin

GD25 cells which were deficient in the β_1 subunit of integrin (Fässler et al. 1995) and GD25-β1A cells which were stable transfected with the splice variant A of the β_1 subunit (Wennerberg et al. 1996) were kindly provided by Dr. Reinhard Fässler. The cells were grown at 37 °C in 5% CO_2 in 35-mm culture dishes (Falcon/Becton Dickinson, Franklin Lake, NJ) in Dulbecco's modified eagle medium (DMEM, 4500 mg/L D-glucose, with glutamax I, sodium pyruvate) (no. 31966, Gibco, Eggenstein, Germany) supplemented with 10% fetal calf serum (no. 10106, Gibco). The gene of chicken vinculin (Price et al. 1989) in the eukaryotic expression vector pJ4Ω was kindly provided by Dr. Benjamin Geiger. The vinculin cDNA was amplified by PCR and ligated into the multiple cloning site of the pEGFP-C1 expression vector (Clontech, Heidelberg, Germany). The plasmid containing the vinculin cDNA was introduced into GD25-b1A cells by calcium phosphate transfection. The cells were then incubated in fresh medium with 10% serum for about 16 h until high expression of the fusion protein was attained. For all measurements the transfected cells were treated with trypsin/EDTA (no. 35400, Gibco), resuspended in serum-containing medium to inactivate the trypsin, and washed twice by centrifugation in PBS. The cells were resuspended in serum-free DMEM (about 2×10^4 cells/mL) and cultivated on a silicon chip in a tissue culture dish (Falcon) at 37 °C for 1–6 h. Then the cells were stained with DiI. In some experiments the culture medium contained 0.5 mg/mL of the peptide GRGDS (A5686, Sigma) and the cells were cultured for 2–3 h before staining.

We checked the distribution of vinculin by immunostaining after fixation with paraformaldehyde (2% in PBS) for 15 min at 4 °C. The fixated cells were washed three times for 10 min with PBS and permeabilized with Triton X-100 (0.1% in PBS) for 15 min. After blocking with 1% BSA in PBS for 30 min, an antibody against mouse vinculin (provided by Dr. Reinhard Fässler) was added. After 90 min of incubation, the chips were washed three times for 10 min with PBS followed by incubation with Cy3-conjugated antibody against mouse immunoglobulin (Jackson ImmunoResearch Laboratories, West Grove, Pa.) for 1 h, and subsequently washed three times for 10 min with PBS.

Substrate

To apply FLIC microscopy, we cultured the cells on silicon chips. We oxidized 4-inch silicon wafers (100 surface) at 1000 °C in wet oxygen to obtain 160 nm of homogeneous oxide. A surface with four levels of oxide with quadratic terraces of 5 μm × 5 μm was fabricated by photolithography and HF etching (Braun and Fromherz 1997). The wafers were cut into 10 mm × 35 mm chips and cleaned by soaking in H_2SO_4 and H_2O_2 (volume ratio 3:1) for 15 min. After hydrophobic coating (2% dimethyldichlorosilane in toluol for 15 min), the height of the steps was measured by ellipsometry on larger reference squares to an accuracy of 0.3 nm. The chips were sterilized by UV illumination. They were coated by incubating in PBS with 10 μg/mL of human fibronectin (F2006, Sigma, Heidelberg, Germany) or 10 μg/mL of laminin-1 (kindly provided by Dr. Rupert Timpl) overnight at 4 °C in a 35-mm diameter dish. The dried fibronectin film corresponded optically to a 2.2-nm layer of silicon dioxide (refractive index 1.46) as determined by ellipsometry, the dried laminin film to 4-nm oxide. After coating with fibronectin or laminin, the surface was blocked with 1% BSA in PBS for 2–3 h and washed with PBS (Aumailley et al. 1989).

Staining

Shortly before the fluorescence measurements, the culture medium was replaced by an aqueous dispersion of the amphiphilic cyanine dye DiI (Molecular Probes, Eugene, Ore.) in 0.05 M Tris buffered saline (pH 7.4). The dispersion was made by adding 2 μL of 2.5 mM ethanolic solution of the dye to 3 mL buffer (Braun and Fromherz 1997). The dye molecules were immediately incorporated into the plasma membrane to give a homogenous staining. DiI has been used in TIRF microscopy (Axelrod 1981) and in many in vivo studies of embryonal development of neurons (Thanos and Bonhoeffer 1987; Steljes et al. 1999). It distributes in the membrane through rapid diffusion. The transition dipole of excitation and emission is parallel to the cell membrane (Axelrod 1979). The flip-flop of the dye from one side of the membrane to the other side is slow (Wolf 1985). A significant internalization into the cytoplasm occurs only after 1 h. It is indicated by the disappearance of the typical checkerboard pattern of fluorescence on the silicon chips with oxide terraces which is caused by the dye in the attached

plasma membrane (see below), and by the appearance of a high and inhomogeneous background fluorescence. For that reason, all measurements were completed within 30 min after staining.

Fluorescence microscopy

Fluorescence was observed with a water immersion objective (100 ×, numerical aperture 1.0, Axioskop, Zeiss, Oberkochen) using a Xenon lamp (Zeiss). The fluorescence of GFP was excited with a bandpass filter 470/40 nm (AHF Analysentechnik, Tübingen) through a dichroic beamsplitter (Q495LP, AHF). The emission was detected through a bandpass filter (HQ510/20M, AHF). The dye DiI was excited monochromatically at 546 nm through a dichroic mirror (Q565LP, AHF) and a bandpass filter (546/10 nm, 546FGS, Andover, Salem, NH). The same conditions were chosen for immunofluorescence with Cy3. All fluorescence images were obtained with a CCD camera with 752 × 582 pixels (Sony chip ICX039AL, HRYX, Theta System, Munich).

FLIC microscopy

FLIC microscopy was introduced in previous papers (Lambacher and Fromherz 1996; Braun and Fromherz 1997). In short, standing modes of light exist in front of the reflecting surface of silicon. As a consequence, both the excitation and the fluorescence emission of a dye depend on the distance from the silicon. A set of four oxide terraces brings the stained membrane of an adhering cell to defined distances from the mirror given by the known thickness of the oxide d_{ox} and the unknown distance d_{cleft} between the lower membrane and the oxide, as illustrated by Fig. 1. The four fluorescence intensities (average and standard deviation) are measured and plotted versus the height of the terraces, which are identified by their contrast in reflected light. The data are compared with an electromagnetic theory that takes into account all directions, polarizations and wavelengths of the incident light and of the emitted light, the interaction of the electromagnetic field with the silicon chip, and the interaction with the dye as defined by its absorption and fluorescence spectra and the orientations of its transition moments. The detected intensity J_{fl} depends on the probability per unit time of excitation P_{ex}, on the transition probabilities of deactivation by the interaction with the electromagnetic field k_{elmag} and by intramolecular internal conversion k_{ic}, and on the probability per unit time of emission P_{em} into the detector according to Eq. (1) (Lambacher and Fromherz 1996):

$$J_{fl} = P_{em} \frac{1}{k_{elmag} + k_{ic}} P_{ex} \quad (1)$$

The variation of k_{elmag} due to effects of the far and near field of the radiating dye (Kuhn 1970; Tews 1973; Drexhage 1974; Chance et al. 1975) plays a minor role if DiI is above 10 nm from the silicon surface, as shown by comparison of theory and experiment (Lambacher and Fromherz 1996; Lambacher and Fromherz, in preparation). We fitted the intensity data of cell adhesion according to Eq. (2) with a simplified function $F(d_{ox}, d_{cleft}) \propto P_{em}P_{ex}$ using three parameters: the distance d_{cleft}, a scaling factor a, and a constant background level b (Lambacher and Fromherz 1996; Braun and Fromherz 1997, 1998):

$$J_{fl} = a \cdot F(d_{ox}, d_{cleft}) + b \quad (2)$$

Prerequisites of the FLIC method are (1) homogeneous staining and illumination and (2) existence of homologous regions of cell adhesion on all four oxide terraces. When the microscope is focused on the attached membrane, perturbations by the upper membrane are negligible if its separation is larger than 0.5 μm because the standing waves level out, mainly owing to the large numerical aperture of the microscope. Problems arise only in flat regions of the cells when the upper membrane is rough and cannot be recognized by interference fringes (Braun and Fromherz 1997). The estimated precision of the average distance d_{cleft} due to systematic and stochastic errors is around 1 nm, independent of its absolute value as discussed in previous studies (Braun and Fromherz 1997, 1998). The lateral resolution is approximately 400 nm.

Distance maps were evaluated on selected terraces by solving Eq. (2) for d_{cleft} after determination of a and b on homologous subsquares (Braun and Fromherz 1998). This process is most precise at high values of the slope $dF(d_{ox}, d_{cleft})/dd_{cleft}$. The intensity contrast due to height variation is inverted with the sign of this slope: if positive, increased intensity means increased distance; if negative, increased intensity means decreased distance. This inversion in contrast enables distinguishing the distance evaluation from an intensity variation due inhomogeneous staining.

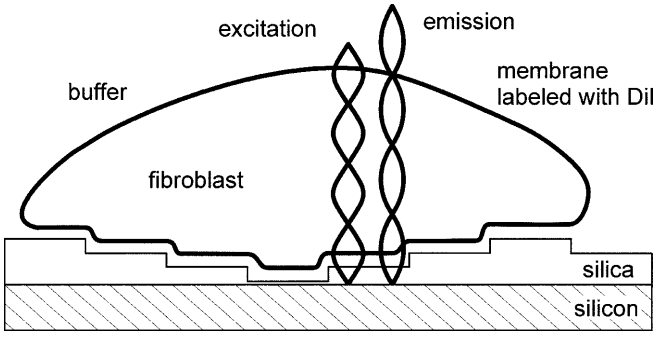

Fig. 1 Fluorescence interference contrast (FLIC) microscopy. Schematic illustration of FLIC microscopy on a silicon chip (not to scale). A fibroblast grows across microscopic terraces of silica coated with fibronectin. The height of the steps is about 50 nm, their width is 5 μm. The cell membrane is stained with a fluorescent dye. The fluorescence intensity of the attached membrane depends on the distance from the reflecting silicon owing to standing modes of light which affect the excitation and the emission of the dye. That distance depends on the height d_{ox} of the terraces and on the distance d_{cleft} between the surface and the membrane. Contributions from the upper side of the cell are avoided by the focus at a large aperture of the microscope. The distance d_{cleft} is determined by fitting the fluorescence intensities on four different terraces by an electromagnetic FLIC theory

Results

Smooth area of cell adhesion

We cultured GD25-β1A cells on a silicon chip with 5 μm × 5 μm terraces of silica with four different heights: $d_{ox} = 17.0$, 57.0, 105.7, and 147.9 nm. The surface was coated with fibronectin or laminin and blocked with 1% BSA. A fluorescence micrograph of a cell attached to fibronectin stained with DiI is shown in Fig. 2A together with a reflection micrograph for the assignment of the four silica terraces in Fig. 2B. (The intensity contrast due to cell structure seen in reflected light is visible only with a closed Abbé condenser. It does not affect the intensity of fluorescence recorded with an open condenser.) We observed a checkerboard pattern of the fluorescence in register with the quadratic steps of silica. The fluorescence was dark on the first oxide, bright on the second, intermediate on the third, and the darkest on the fourth oxide. The intensity was identical on homologous steps of equal oxide thickness and was rather homogeneous

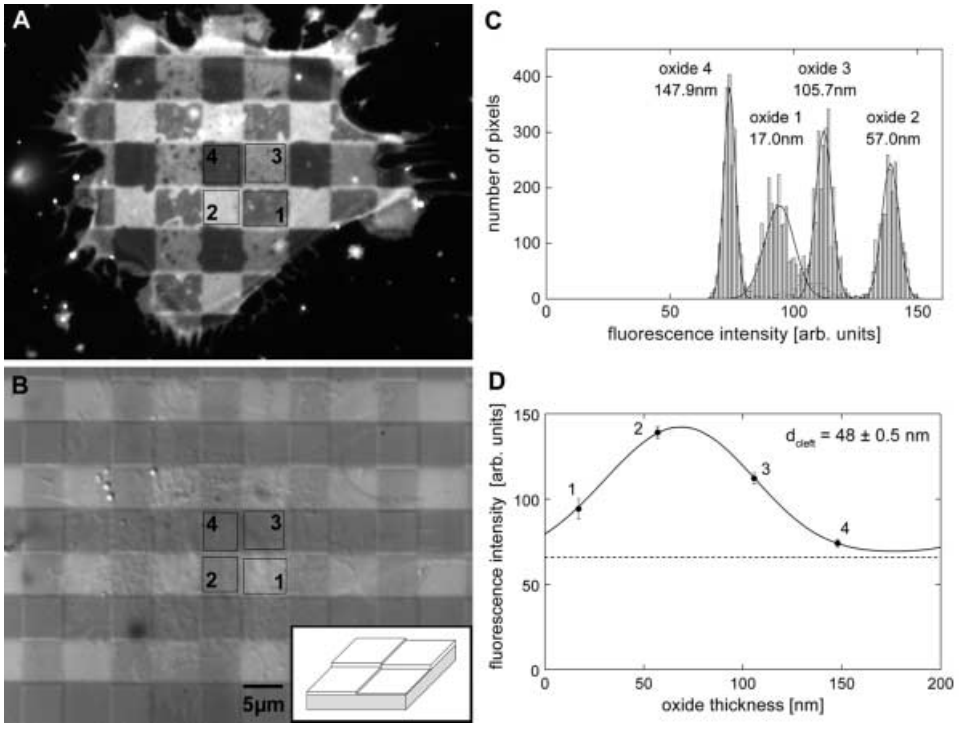

Fig. 2A–D Distance of fibroblast on fibronectin. **A** Fluorescence micrograph of a GD25-β1A cell stained with the dye DiI. The silicon substrate is covered with 5 µm × 5 µm terraces of silicon dioxide (height 17.0 nm, 57.0 nm, 105.7 nm, 147.9 nm) which are coated with fibronectin. **B** Reflection micrograph with closed Abbé condenser used to assign the terraces 1, 2, 3, and 4 as sketched in the *insert*. **C** Histograms of intensities on the terraces 1, 2, 3, and 4 fitted by Gaussians. **D** Average and standard deviation of intensity versus height of the oxide terraces. The data are fitted by the FLIC theory with an average distance between membrane and substrate $d_{\text{cleft}} = 48 \pm 0.5$ nm

on each square. Some bright spots were observed on oxide no. 1 and some dark spots on oxide no. 3, both with diameters around 500 nm.

Histograms of the intensities on four selected steps were evaluated and fitted by Gaussians as shown in Fig. 2C. Average and standard deviation were plotted versus the height d_{ox} of the steps in Fig. 2D. We fitted the data points with the radiative approximation of the FLIC theory. From the fit we obtained the average distance and its statistical error as $d_{\text{cleft}} = 48 \pm 0.5$ nm. For a population of cells the average distance was in the range between 40 nm and 60 nm ($d_{\text{cleft}} = 48 \pm 0.5$ nm, $N = 360$).

The identical brightness on homologous terraces indicated that the distance of the cell membrane was rather homogenous from terrace to terrace. The width of the histograms of intensity in Fig. 2C may be due to a variability of the distance d_{cleft} (roughness) and of staining. From the standard deviations of the histograms we estimated an upper limit of ± 5 nm of the roughness using FLIC theory. The patches in Fig. 2A – which are bright on oxide no. 1 and dark on oxide no. 3 – indicate an upward bulging of the membrane, considering the position of the average intensities on the interference curve in Fig. 2D and the corresponding slope.

On fibronectin, we found no difference in the average distance between the ventral cell membrane for GD25 cells with $\alpha_V\beta_3$ integrin receptors and for GD25-β1A cells with additional $\alpha_5\beta_1$ integrin receptors. There was also no difference between GD25-β1A cells in the absence or presence of GRGDS that blocks the RGD binding site of $\alpha_V\beta_3$ integrin, i.e a change of the integrin-fibronectin interaction – from $\alpha_V\beta_3$-fibronectin to $\alpha_5\beta_1$-fibronectin or from the $\alpha_V\beta_3$-RGD site to the $\alpha_V\beta_3$-PHSRN site (Grant et al. 1997), respectively – does not affect the average separation of cell and surface.

GFP-vinculin

We used vinculin as a marker to localize focal complexes (Geiger 1979; Avnur and Geiger 1981). In order to identify the position of focal contacts in situ under the conditions of the distance measurement, we labeled vinculin with GFP. A fluorescence micrograph of a GD25-β1A cell which was transfected with a fusion construct of vinculin and GFP is shown in Fig. 3A. Well-defined patches of fluorescence were seen throughout the area of cell adhesion. As a control, we performed an immunostaining against vinculin as shown in Fig. 3B. The antibody staining revealed the typical shape and distribution of focal contacts (Geiger 1979), as was described previously for GD25 and GD25-b1A cells without GFP fusion (Fässler et al. 1995; Wennerberg et al. 1996). The pattern of immunostaining matched the pattern of GFP in all details. The experiment demonstrated that the GFP label does not perturb the formation of focal contacts and that GFP-vinculin is able to visualize focal contacts in situ.

The fluorescence of GFP-vinculin is also modulated by the FLIC effect. Both in Fig. 4B and C we find an intense and similar GFP-vinculin fluorescence on the oxide terraces 1 and 2, but only a low GFP-vinculin fluorescence on the terraces 3 and 4. The patches of GFP

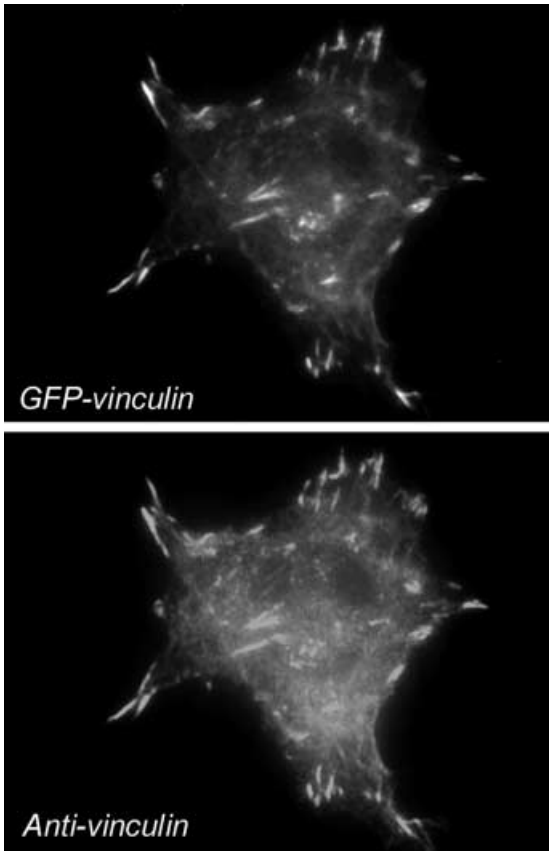

Fig. 3 Distribution of vinculin. The GD25-β1A cell was transfected with a GFP-vinculin fusion construct and cultivated on a homogeneously oxidized silicon chip coated with fibronectin. *Top*: in situ fluorescence of green fluorescent protein (GFP). *Bottom*: immunostaining with anti-vinculin and a Cy3-labeled anti-immunoglobulin antibody after fixation

did not exhibit a well-defined FLIC checkerboard pattern such as DiI, because the brightness of the patches on different terraces was not identical and because an inhomogeneous GFP background in the cytoplasm blurred the FLIC pattern. Nonetheless, we tried to estimate the position of GFP by photometry of several patches on the four terraces and by comparison with the FLIC theory, assuming a random orientation of the transition moment. We obtained a distance of $d_{\text{cleft}} = 48 \pm 0.5$ nm between GFP-vinculin and the substrate. Thus GFP-vinculin is located well above the plasma membrane as expected. The approach indicates that FLIC microscopy may be used to determine the distance of a specific protein from the substrate and the membrane in a living cell.

Distance maps

We correlated the distance between membrane and substrate with the sites of focal adhesion by taking two fluorescence micrographs, one in the light of GFP and the other in the light of DiI. Three GD25-β1A cells are shown in Fig. 4 with increasing expression of GFP-vinculin. The GFP tag revealed dot-like vinculin spots in Fig. 4A, ellipsoidal focal contacts in Fig. 4B, and aligned elongated focal contacts in Fig. 4C. The dominating feature of the corresponding FLIC micrographs in Fig. 4D–F was the distinct checkerboard pattern on the oxide terraces in all three cases. The quadratic areas were most homogeneous in Fig. 4D. Bright and dark perturbations appeared as in Fig. 4E in regions where vinculin was accumulated. A parallel texture appeared in Fig. 4F aligned with the vinculin stripes. The three cells shown in Fig. 4 are representative for the fibroblasts studied in this investigation. We found no significant difference with respect to the expression of GFP-vinculin or with respect to the pattern of FLIC microscopy between GD25 cells and GD25-β1A cells without and with the GRGDS peptide in the bath.

To determine the profile of cell adhesion in the area of focal contacts, we selected five typical regions in the three cells of Fig. 4 as marked by (a), (b), (c), (d), and (e). There we computed a complete distance map. The results are shown in the five picture pairs in Fig. 5 with color coding of distance. The evaluation of distance maps was restricted to the oxide terraces 1 and 3 (Fig. 3A). Only there the slope of the intensity function was sufficient to obtain a proper scaling (Fig. 3D). Enhanced brightness indicated upward bulging on oxide 1, and downward bulging on oxide 3. This distance map had an error of approximately 5 nm. The most significant feature in all five selected areas was a dominating plateau around 50 nm (green color). Based on this distance, various features of roughness were observed in the five selected areas by (a), (b), (c), (d), and (e).

We observed a single circular vinculin spot in area (a) with a diameter of about 500 nm. With respect to distance, the whole area of 5 μm × 5 μm was rather homogeneous with $d_{\text{cleft}} \approx 50$ nm. There were a few discrete spots where the distance was smaller, with $d_{\text{cleft}} \approx 15$ nm. The picture illustrated that regions of close contact exist, but that they are not related to focal contacts as tagged by vinculin.

There was a single ellipsoidal vinculin spot at the upper edge of area (b). With respect to distance, the whole square of 5 μm × 5 μm was rather inhomogeneous with extended upward bulging up to 70 nm and downward bulging down to 15 nm. These features of rough adhesion occurred in a region without focal adhesion. In particular, the areas of close contact were not related with the presence of vinculin.

A single ellipsoidal vinculin spot was seen also in region (c). Again the distance was rather inhomogeneous in the whole square of 5 μm × 5 μm with upward bulging up to 100 nm. There was a downward bulging down to 15 nm at the bottom. Part of it matched the area of focal contact, part of it was parallel to it.

Many parallel stripes of focal contacts appeared in region (d). There the distance was rather homogeneous

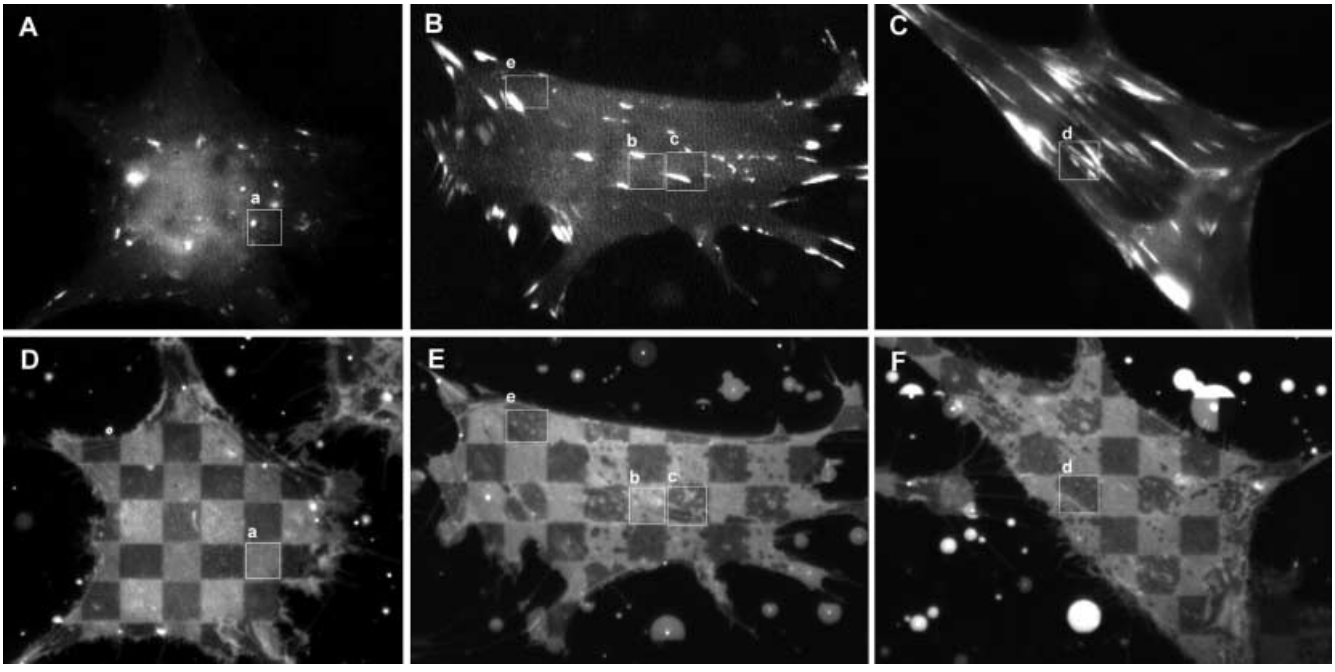

Fig. 4A–F Correlation of vinculin-GFP and FLIC microscopy with DiI. Fluorescence micrographs of three GD25-β1A cells cultured for 3 h. **A–C**: fluorescence of GFP-vinculin fusion. **D–F**: fluorescence of DiI on silicon with 5 μm × 5 μm oxide terraces. The areas selected for a computation of distance maps are marked with *a* (terrace 3), *b* (terrace 2), *c* (terrace 1), *d* (terrace 1), and *e* (terrace 1)

at about $d_{\text{cleft}} \approx 50$ nm. The distance map was dominated by a streak of upward bulging of 80 nm in the left lower corner that was oriented in parallel to the focal contacts in the right upper corner. Striking features were the discrete spots with upward bulging. A single spot of close contact was observed, but its shape did not correlate with the shape of the vinculin patch.

A large vinculin spot was present in the left lower corner of region (e). Here we observed a close contact of about 25 nm that matched the area of focal contact. The rest of the area without vinculin is dominated by dot-like upward bulging.

In summary, we found no correlation between the expression of vinculin which marks focal adhesion and a close contact between the plasma membrane and the substrate coated with fibronectin.

Laminin

For comparison, the correlation study was repeated for laminin. GD25-β1A cells on laminin neither formed vinculin patches nor exhibited membrane deformation within 2 h of culture (Fig. 6). After 2 h the membrane became rough but the vinculin still appeared diffuse with occasional fine patches at the cell periphery and in the cell body. In agreement with the previous study done

Fig. 5a–e Correlation of vinculin and distance. Five areas are selected from the three cells shown in Fig. 4. *Top*: fluorescence of GFP-vinculin fusion. *Bottom*: color-coded distance map based on the fluorescence of DiI

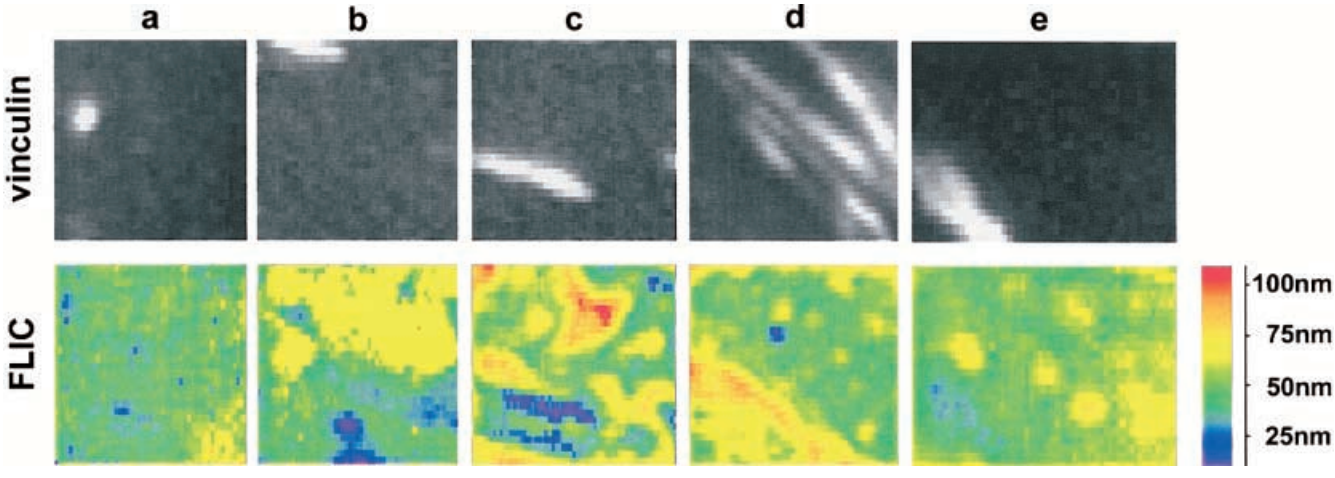

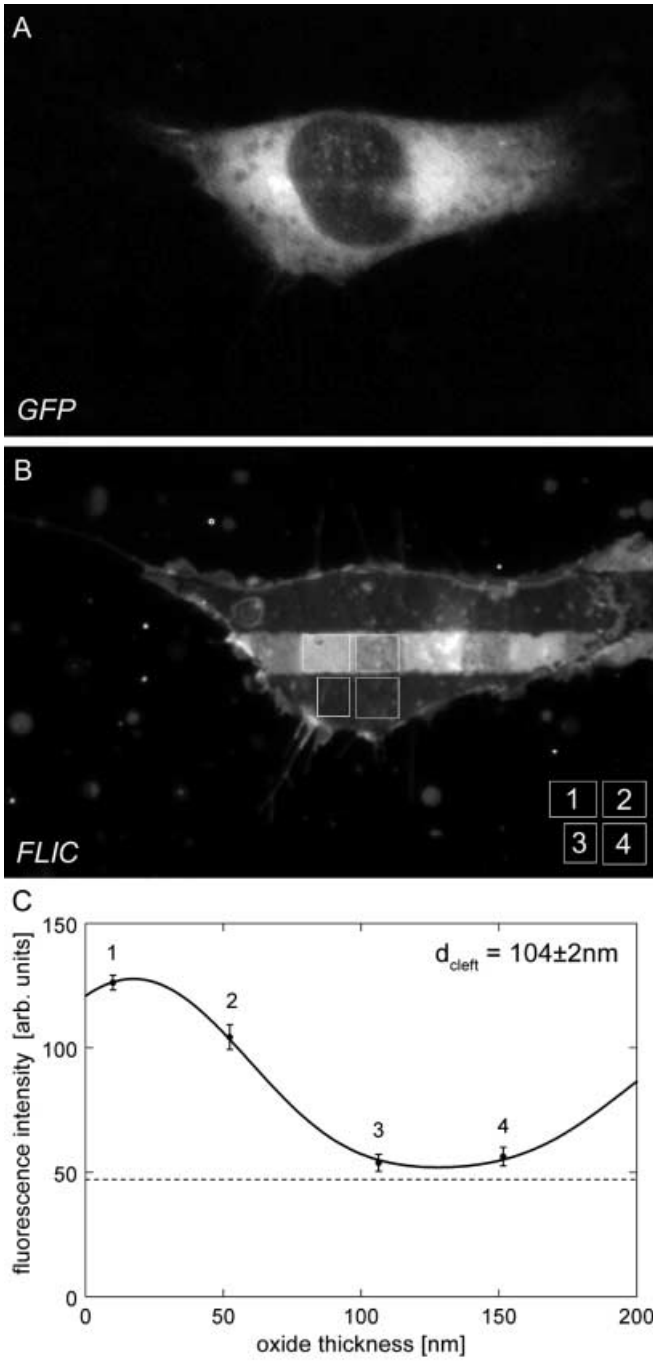

Fig. 6A–C Adhesion on laminin. GD25-β1A cells were cultured for 1 h on silicon with 5 μm × 5 μm oxide terraces coated with laminin. **A** Fluorescence of GFP-vinculin. No patches of vinculin are formed. **B** Fluorescence of DiI. There are no significant local deformations of the membrane. **C** Intensity of selected areas of **B** versus oxide thickness. The data are fitted by the FLIC theory with an average distance $d_{\text{cleft}} = 48 \pm 0.5$ nm between membrane and substrate

with IRM (Regen and Horwitz 1992), the FLIC micrograph showed no close contacts. The effective adhesion of GD25-b1A cells to laminin without the presence of focal contacts implicates an additional type of interaction with the extracellular matrix protein.

Discussion

Adhesion and focal contact

Adhesion of GD25 cells on fibronectin is dominated by a plateau with a distance of about 50 nm. On this background there are various features of roughness with upward bulging up to 120 nm and close adhesion down to 15 nm. In general, the roughness increases with the overall expression of vinculin, i.e. with the increasing formation of focal contacts. However, there is no correlation of the local features of the distance map with the distribution of vinculin. Focal adhesion is not identical with close adhesion.

A fibronectin dimer molecule is about 120 nm long (Engel et al. 1981). Integrin molecules protrude on the extracellular side by about 15 nm from the membrane (Nermut et al. 1988; Erb et al. 1997). Thus a distance of 50 nm between membrane and substrate can be bridged easily by filaments of fibronectin, even if the average thickness of a dry film is only 2.2 nm. Adsorbed fibronectin molecules may form a cushion which keeps the membrane at a distance of about 50 nm by the effect of a steric force of dangling molecules (Zeck and Fromherz, unpublished). Some of these molecules bind to the focal complex in a receptor equilibrium. The existence of a focal contact – its mechanical strength and its efficiency of transmembrane signaling – are determined by the local specific binding constant, by the number and strength of the molecular links, and by the physical state of fibronectin (Katz et al. 2000). A deformation of the membrane is not required, either from a structural or from a functional point of view.

A particular feature of cell adhesion on fibronectin is the appearance of defined upward bulging with a diameter of a few hundred nanometers. They appear particularly in areas without vinculin. These spots may be assigned tentatively to point contacts as described for neuronal cells (Renaudin et al. 1999). Recent studies have shown also novel adhesion structures in the absence of vinculin called fibrillar adhesions (Zamir et al. 2000). At present moment we are not able to discuss the mechanism that causes the deformation of the membrane in regions without vinculin clusters. Detailed investigation with other GFP-tagged adhesion molecules will be necessary.

Comparison with IRM

IRM (Curtis 1964) reveals black spots in fibroblasts which co-localize with regions of focal adhesion as visualized by immunostaining (Izzard and Lochner 1976; Geiger 1979). We checked that there is a perfect correlation of low reflection in IRM and of the distribution of GFP-vinculin in GD25 and GD25-β1A cells under the conditions of our experiment. The coincidence of focal adhesion and black spots in IRM is interpreted generally

in terms of a very close contact of membrane and substrate. This interpretation relies on the assumption that the contrast of IRM is dominated by the destructive interference of light reflected from the bottom of the cell and from the top of the substrate (Izzard and Lochner 1976). However, it has been pointed out in the past that reflection from dense material on the cytoplasmic side of the membrane may contribute significantly (Heath and Dunn 1978; Bailey and Gingell 1988). In fact such an enhanced effective thickness of the membrane exists at a focal contact due the intracellular protein complex. Thus IRM is able to detect sensitively the position of a focal contact, but it does not probe the width of the cleft between membrane and substrate.

To demonstrate the problem with IRM and to compare it with FLIC microscopy, we computed the reflection intensity of IRM and the fluorescence intensity of FLIC as a function of the membrane-substrate distance and of the membrane thickness. For unpolarized Köhler illumination, the reflected intensity is proportional to the sum of the squared reflection coefficients r of TE and TM polarizations at the wavelength $\lambda = 546$ nm according to Eq. (3) integrated over the polar angle ϑ up to $\vartheta_M = 55.4°$ at a numerical aperture NA = 1.25:

$$I \propto \int \left[|r_{TE}(\vartheta)|^2 + |r_{TM}(\vartheta)|^2 \right] \sin \vartheta \, d\vartheta \qquad (3)$$

We considered a layer system of glass (refractive index $n = 1.518$), a cleft ($n = 1.333$), an attached membrane (thickness $d = 4$ nm, $n = 1.45$), cytoplasm ($d = 3.0$ μm, $n = 1.37$), an upper membrane ($d = 4$ nm, $n = 1.45$), and medium ($n = 1.333$). The intensity was normalized to the reflected intensity from the pure glass substrate, giving a relative intensity $RI = I_{cell}/I_{glass}$. Figure 7A illustrates the resulting ambiguity of IRM: starting at a membrane thickness of 4 nm and a membrane-substrate distance of 50 nm, the relative intensity is lowered by closer adhesion of the attached membrane at constant thickness as well as by an enhanced thickness at constant distance. IRM is not able to distinguish a reduced distance from a thicker membrane. For comparison, an intensity map is shown in Fig. 7B for FLIC microscopy on a chip without oxide. Here the signal is quite insensitive to a thickening of the attached membrane. The maximal decrease in the fitted distance was 2.7 nm when the lower membrane thickness was varied. It must be noted that FLIC relies on a fit of the intensities on several oxide terraces, and only a shift of the complete intensity curve in Fig. 7B leads to a change of the fitted distance.

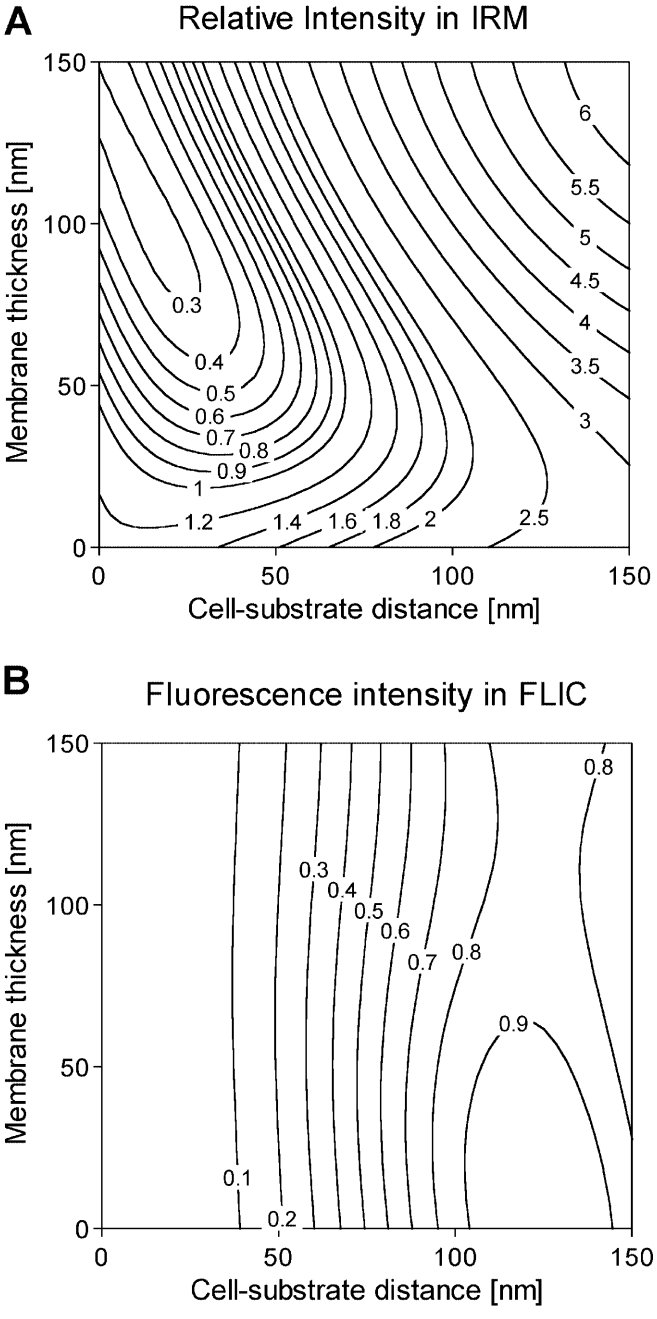

Fig. 7A, B Model calculations for IRM and FLIC microscopy. The normalized reflection intensity and the relative fluorescence intensity are plotted versus the cell-substrate distance and versus the thickness of the lower membrane to model intracellular protein complexes. **A** The normalized intensity of IRM shows a strong dependence on both the membrane thickness and the cell-substrate distance. **B** The fluorescence intensity of FLIC barely depends on the membrane thickness

Comparison with other methods

TIRF and TIRAF microscopy rely on a labeling of the cell membrane or of the extracellular space between the membrane and the surface by a fluorescent dye (Truskey et al. 1992; Geggier and Fuhr 1999). The fluorescence is observed under conditions of total reflection. Roughness of cell adhesion has been described (Lanni et al. 1985; Burmeister et al. 1994). A correlation of close adhesion to focal adhesion was reported on an uncoated substrate (Lanni et al. 1985). A preliminary study indicates that there also exists a correlation of TIRAF contrast and GFP-vinculin on a fibronectin substrate (Iwanaga, Geggier, Fuhr and Fromherz, in preparation). However,

TIRAF contrast is most sensitive to the optical parameters and a dark contrast may indicate a minute change of the refractive index of the extracellular cleft.

Close adhesion was observed in cross sections of fixed and embedded samples by TEM with cells on a gelatin substrate (Chen and Singer 1982). Fixation with glutaraldehyde/paraformaldehyde and embedding in an organic resin may affect the region of focal adhesion and the rest of the membrane differently, if filaments connect substrate and integrin in the region of focal adhesion. Artifacts of local contraction may be formed. It will be important to correlate similar measurements directly with FLIC experiments, avoiding possible artifacts of electron microscopy.

Plaques with proteins from the focal complex were observed when fibroblasts were detached from the substrate (Avnur and Geiger 1981; Lark et al. 1985). These observations indicate strong attractive forces between membrane and substrate, but they do not indicate a structure of close adhesion. They are compatible with focal complexes that bind to the substrate by filaments of fibronectin.

Conclusion

Focal contacts are specialized areas of the plasma membrane with respect to a local interactions with the substrate. We have shown that focal contacts – defined by an accumulation of vinculin – are not related with a close contact of fibroblasts on fibronectin under standard conditions of cell culture. An increasing formation of focal contacts leads to an enhanced roughness of the attached membrane. Areas of close contact exist, but they do not correlate with focal adhesion. An effective interaction of fibronectin with integrins – which leads to mechanical attraction and transmembrane signaling – does not require a structure of close adhesion. It can well be mediated by a receptor equilibrium with a cushion of dangling molecules of extracellular matrix proteins.

Acknowledgements We thank Reinhard Fässler for the GD25 and GD25-β1A cells and for many helpful discussions, Benjamin Geiger for the vinculin gene, Jürgen Kupper and Elisabeth Meyer for advice with molecular biology. We are grateful to Igor Weber and Hermine M. Hitzler-Alimoradian for their help with IRM and Peter Geggier and Günther Fuhr for a cooperation on TIRAF measurements. The project was supported by the Bundesministerium für Bildung und Forschung.

References

Alberts B, Bray D, Lewis J, Raff M, Roberts K, Watson JD (1989) Molecular biology of the cell, 2nd edn. Garland, New York, p 635

Aumailley M, Mann K, Mark H, Timpl R (1989) Cell attachment properties of collagen type VI and Arg-Gly-Asp dependent binding to its α2(VI) and α3(VI) chains. Exp Cell Res 181: 463–474

Avnur Z, Geiger B (1981) Substrate-attached membranes of cultured cells, isolation and characterization of ventral cell membranes and the associated cytoskeleton. J Mol Biol 153:361–379

Axelrod D (1979) Carbocyanine dye orientation in red cell membrane studies by microscopic fluorescence polarization. Biophys J 26:557–573

Axelrod D (1981) Cell-substrate contacts illuminated by total internal reflection fluorescence. J Cell Biol 89:141–145

Bailey J, Gingell D (1988) Contacts of chick fibroblasts on glass: results and limitations of quantitative interferometry. J Cell Sci 90:215–224

Braun D, Fromherz P (1997) Fluorescence interference-contrast microscopy of cell adhesion on oxidized silicon. Appl Phys A 65:341–348

Braun D, Fromherz P (1998) Fluorescence interferometry of neuronal cell adhesion on microstructured silicon. Phys Rev Lett 81:5241–5244

Burmeister JS, Truskey GA, Reichert WM (1994) Quantitative analysis of variable-angle total internal reflection fluorescence microscopy of cell/substrate contacts. J Microsc 173:39–51

Burmeister JS, Olivier LA, Reichert WM, Truskey GA (1998) Application of total internal reflection fluorescence microscopy to study cell adhesion to biomaterials. Biomaterials 19:307–325

Chance RR, Prock A, Silbey R (1975) Comments on the classical theory of energy transfer. J Chem Phys 62:2245–2253

Chen W, Singer SJ (1982) Immunoelectron microscopic studies of the sites of cell-substratum and cell-cell contacts in cultured fibroblasts. J Cell Biol 95:205–222

Curtis AS (1964) The mechanism of adhesion of cells to glass. A study by interference reflection microscopy. J Cell Biol 20: 199–215

Drexhage KH (1974) Interaction of light with monomolecular dye layers. Prog Opt 12:163–232

Engel J, Odermatt E, Engel A, Madri JA, Furthmayr H, Rohde H, Timpl R (1981) Shapes, domain organizations and flexibility of laminin and fibronectin, two multifunctional proteins of the extracellular matrix. J Mol Biol 150:97–120

Erb EM, Tangemann K, Bohrmann B, Müller B, Engel J (1997) Integrin alphaIIb beta3 reconstituted into lipid bilayers is nonclustered in its activated state but clusters after fibrinogen binding. Biochemistry 36:7395–7402

Fässler R, Pfaff M, Murphy J, Noegel AA, Johansson S, Timpl R, Albrecht R (1995) Lack of b1 integrin gene in embryonic stem cells affects morphology, adhesion and migration but not integration into the inner cell mass of blastocysts. J Cell Biol 128:979–988

Geggier P, Fuhr G (1999) A time-resolved total internal reflection aqueous fluorescence (TIRAF) microscope for the investigation of cell adhesion dynamics. Appl Phys A 68:505–513

Geiger B (1979) A 130 K protein from chicken gizzard: its localization at the termini of microfilament bundles in cultured chicken cells. Cell 18:193–205

Gingell D, Heavens O (1996) Elimination of the effects of stray light in measurements by total internal reflection aqueous fluorescence (TIRAF). J Microsc 182:141–148

Gingell D, Todd I (1979) Interference reflection microscopy: a quantitative theory for image interpretation and its application to cell-substratum separation measurement. Biophys J 26: 507–526

Grant RP, Spitzfaden C, Altroff H, Campbell ID, Mardon HJ (1997) Structural requirements for biological activity of the ninth and tenth FIII domains of human fibronectin. J Biol Chem 272:6259–6266

Heath JP, Dunn GA (1978) Cell to substratum contacts of chick fibroblasts and their relation to the microfilament system. A correlated interference-reflection and high-voltage electron-microscope study. J Cell Sci 29:197–212

Izzard CS, Lochner LR (1976) Cell-to-substrate contacts in living fibroblasts: an interference reflexion study with an evaluation of the technique. J Cell Sci 21:129–159

Katz B-Z, Zamir E, Bershadsky A, Kam Z, Yamada KM, Geiger B (2000) Physical state of the extracellular matrix regulates the

structure and molecular composition of cell-matrix adhesions. Mol Biol Cell 11:1047–1060

Kuhn H (1970) Classical aspects of energy transfer in molecular systems. J Chem Phys 53:101–108

Lambacher A, Fromherz P (1996) Fluorescence interference-contrast microscopy on oxidized silicon using a monomolecular dye layer. Appl Phys A 63: 207–216

Lanni F, Waggoner AS, Taylor DL (1985) Structural organization of interphase 3T3 fibroblasts studied by total internal reflection fluorescence microscopy. J Cell Biol 100:1091–1102

Lark MW, Laterra J, Culp LA (1985) Close and focal contact adhesion of fibroblasts to a fibronectin-containing matrix. Fed Proc 44:394–403

Nermut MV, Green NM, Eason P, Yamada SS, Yamada KM (1988) Electron microscopy and structural model of human fibronectin receptor. EMBO J 7:4093–4099

Price GJ, Jones P, Davison MD, Patel B, Bendori R, Geiger B, Critchley DR (1989) Primary sequence and domain structure of chicken vinculin. Biochem J 259:453–461

Regen CM, Horwitz AF (1992) Dynamics of b1 integrin-mediated adhesive contacts in motile fibroblasts. J Cell Biol 119: 1347–1359

Renaudin A, Lehmann M, Girault J-A, McKerracher L (1999) Organization of point contacts in neuronal growth cones. J Neurosci Res 55:458–471

Richardson PD, Steiner M (1995) Principles of cell adhesion. CRC Press, Boca Raton

Steljes TP, Kinoshita Y, Wheeler EF, Oppenheim RW, von Bartheld CS (1999) Neurotrophic factor regulation of developing avian oculomotor neurons: differential effects of BDNF and GDNF. J Neurobiol 41:295–315

Tews KH (1973) Zur Variation von Lumineszens-Lebensdauern. Ann Phys 7:97–120

Thanos S, Bonhoeffer F (1987) Axonal arborization in the developing chick retinotectal system. J Comp Neurol 261:155–164

Truskey GA, Burmeister JS, Grapa E, Reichert WM (1992) Total internal reflection fluorescence microscopy (TIRFM). II. Topographical mapping of relative cell/substratum separation distances. J Cell Sci 103:491–499

Wennerberg K, Lohikangas L, Gullberg D, Pfaff M, Johansson S, Fässler R (1996) b1 integrin-dependent and -independent polymerization of fibronectin. J Cell Biol 132:227–238

Wolf DE (1985) Determination of the sidedness of carbocyanine dye labeling of membranes. Biochemistry 24:582–586

Yamada KM, Geiger B (1997) Molecular interactions in cell adhesion complexes. Curr Opin Cell Biol 9:76–85

Zamir E, Katz M, Posen Y, Erez N, Yamada KM, Katz B-Z, Lin S, Lin DC, Bershadsky A, Kam Z, Geiger B (2000) Dynamics and segregation of cell-matrix adhesions in cultured fibroblasts. Nat Cell Biol 2:191–196